System robust optimization of ring resonator-based optical filters

Rehman, Samee; Langelaar, Matthijs

DOI
10.1109/JLT.2016.2568165

Publication date
2016

Document Version
Final published version

Published in
Journal of Lightwave Technology

System Robust Optimization of Ring Resonator-Based Optical Filters

Samee Ur Rehman and Matthijs Langelaar

***Abstract*—Fabrication variations can have a detrimental effect on the performance of optical filters based on ring resonators. However, by using robust optimization these effects can be minimized and device yield can be significantly improved. This paper presents an efficient robust optimization technique for designing manufacturable optical filters based on serial ring resonators. The serial ring resonator is treated as a system which has computationally expensive (directional coupler section) and cheap components (ring section). Cheap mathematical models are constructed of the directional coupler sections in the resonators. The approximate system response based on the cheap model is then robustly optimized. The robust bandpass filter performance is compared against designs that do not take uncertainties into account. The optimality of the robust solutions is confirmed by simulating it on the expensive physical model as a post-processing step. Results indicatethat the employed approach can provide an efficient means for robust optimization of ring resonator-based optical filters.**

***Index Terms*—Design for-manufacturing, expected improvement, integrated optics, Kriging, ring resonators, Robust optimization, system optimization.**

I. Introduction

INTEGRATED photonic devices and systems are prone to manufacturing uncertainties which are an unavoidable aspect of fabrication. If designers do not account for the geometrical variations that can arise in fabrication, the fabricated structure fails to perform according to the designed specifications. Design-for-Manufacturing strategies for integrated photonics therefore have a potential to increase the overall yield and simultaneously reduce the cost of production. However, in order to perform this, information about the capability of the fabrication process is needed. Ideally, designers should have access to data related to the probability distribution of the uncertainties in fabrication. However, such probability data is usually classified and is not disclosed by foundries to external designers. In this case, designers often only know the tolerances of the fabrication process. In other words, the bounds on the fabrication uncertainties are known, but their distribution is unknown.

In the scenario that the uncertainties are bounded-but-unknown [1], robust optimization is an established approach to find a fault-tolerant design. Robust optimization involves finding the best worst-case performance. The design is optimized so that the best performance is achieved given that the worst-case uncertainty with respect to the performance metric is realized. The design found using this method is therefore not insensitive, but has a certain guaranteed minimum performance.

To determine the robust optimum, an iterative optimization process is required. An additional challenge in integrated photonic optimization is that the underlying electromagnetic simulation may be computationally expensive. Repeatedly changing the design parameters and rerunning the simulation to find the optimal design can therefore be prohibitively costly. In order to circumvent this problem, an inexpensive approximate model of the simulation can be constructed and the optimization can be performed on the cheap model. Amongst the available methods for mathematical modeling, Kriging [2] is a strong candidate since it provides an estimator for the approximation error. Using these estimates, the cheap model, otherwise known as a metamodel, can adaptively be improved by simulating the integrated photonic device response in regions of the design domain that are relevant to robust optimization.

The described approximation approach can efficiently find the robust optimum of an integrated photonic device such as an multi-mode interference (MMI) coupler [3], [4] or a single ring resonator [5]. But in order for the approach to be scalable it should also be able to produce a robust solution for large integrated photonic systems consisting of different components.

Research has been performed on finding tolerant designs for different integrated photonic devices [6]–[11]. Similarly, the adverse effects of fabrication variations on the performance of microrings has been exhibited in [12]. However, most of these fault tolerant approaches have been focused on nongeneric methods that only address a particular integrated photonic device. An efficient and scalable approach for robust optimization of integrated photonic *systems* is still lacking. For device level problems, space-mapping [13] is a generic approach for deterministic and nondeterministic optimization of electromagnetic problems. Applications of this approach for optimization of integrated photonic components have also been presented [14]. However, to the best of our knowledge, space-mapping has not been employed for robust optimization of hierarchical systems.

In this work, we propose a system level robust optimization technique for efficiently identifying robust designs for serial ring resonator-based optical filters. A cheap system model is constructed for this purpose based on mathematical models of the components (directional couplers). The approach is not based on a specific physical model. Therefore the method could potentially be employed for robust optimization of other integrated photonic systems. The major restriction is that the structure of the system should be such, that the behavior of the components is independent from one another. This means that e.g. heaters that cause crosstalk between components cannot be

Manuscript received November 09, 2015; revised February 13, 2016 and April 13, 2016; accepted April 14, 2016. Date of publication May 11, 2016; date of current version July 21, 2016.

The authors are with the Precision and Microsystems Engineering, Delft University of Technology, Delft 2628 CD, The Netherlands (e-mail: S.U.Rehman@tudelft.nl; M.Langelaar@tudelft.nl).

Color versions of one or more of the figures in this paper are available online at http://ieeexplore.ieee.org.

Digital Object Identifier 10.1109/JLT.2016.2568165

included. Additionally, it should be recognized that a change in component geometry can cause a local variation in material properties due to stress or shear forces. This change can affect the response of components in the direct vicinity of this local variation in index. In the strict sense, a neighboring component no longer remains independent in this scenario. Fortunately, despite the aforementioned concerns, a number of integrated photonic systems consist of components that are independent, e.g. interferometers based on MMI couplers.

The robust optimum found on the cheap system model should match the result on the reference simulation. To ensure this, the system response is iteratively improved by simulating the underlying components, using a combination of the system level error estimate and the predicted response, in areas that could potentially contain the system robust optimum. We employ a sound mathematical criterion to select the best locations in the design space for refinement, in order to minimize the computational effort of the process.

Serial ring resonator-based optical filters can be seen as examples of integrated photonic systems consisting of several components. Second order and third order serial ring resonators based on single stripe TripleX technology are used for this purpose [15]. Kriging metamodels of the directional coupler sections of the resonators are constructed since simulating the directional coupler is computationally expensive. The suitability of the approach is demonstrated by comparing the robust solution found with the deterministic optimum, i.e., the optimum achieved when optimizing without taking fabrication uncertainties into account.

There has been previous work on optimization of ring resonators based optical filters [16]–[19]. Different approaches have been used for optimization. In [16], the placement of poles and zeros of the transfer function is optimized via trial and error. In [17], a perturbation based approach is employed to vary known mean coupling ratios in order to find the optimal design. However, these methods optimize the filter performance as a function of the coupling ratio of each directional coupler in the system. Optimization is not performed with respect to the geometrical parameters. Uncertainties in the geometry due to fabrication variations are therefore also not taken into account. In the present work, the filter is optimized directly as a function of the geometry, meanwhile the robustness with respect to the variations in geometry is also ensured.

The proposed approach is suited to problems for which the system simulation is cheap and the component behavior is simpler to approximate than the system response. Systems with multiple identical components are especially strong candidates since a single metamodel can then replace the components. Once metamodels have been built for the components, the system is arbitrarily scalable at low computational cost. A library of pre-built component models (the initial samples used here) could be provided in a software package, or built by the user. These pre-built models only need to be refined for each specific case. For instance, once component metamodels are available for expensive to evaluate devices such as directional couplers, MMI couplers, large systems such as interferometers or optical add drop multiplexers consisting of many rings could potentially be robustly optimized at low computational cost.

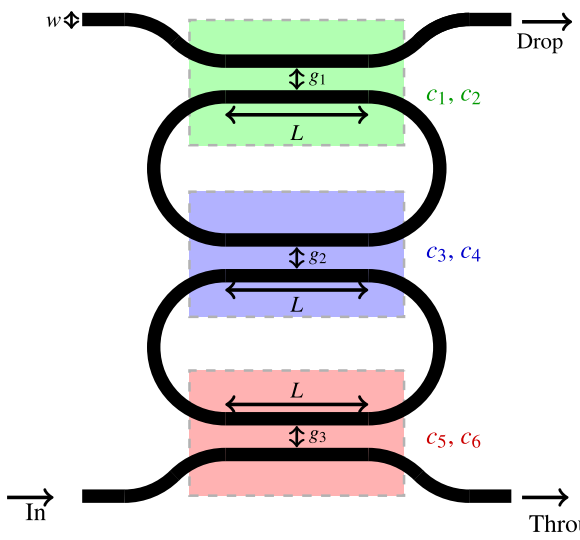

Fig. 1. A second order serial ring resonator is illustrated. The width w, the vector of gaps $\mathbf{g}$ and the length L are the design variables of the problem. The variations in width Δw and in thickness Δt are the uncertainties with respect to which the design has to be robust.

However, the application of the proposed algorithm for robust optimization of other such integrated photonic systems requires further investigation.

II. Application: Serial Ring Resonators

In this work, we are interested in performing robust optimization of optical filters based on serial ring resonators. Fig. 1 shows an illustration of a second-order serial ring resonator. The serial ring resonators are simulated using a single stripe TripleX waveguide [15] with designed thickness of 32 nm. The waveguide basically consists of a stripe of Silicon Nitride buried in Silicon Dioxide. A very small thickness of 32 nm has been chosen for the waveguide since the directional couplers are extremely sensitive to variation at this thickness. This means that if the nominal performance is optimized then even slight variations in the geometry can cause the designed device to not operate as expected. This setting enables better demonstration of both the value as well as the difficulty of performing robust optimization on sensitive systems. The operating wavelength of $\lambda = 637$ nm is also chosen with the motivation that the directional couplers are quite sensitive to variations at this wavelength.

The design variables of the problem are the gaps, g_1 to g_n between the n directional couplers, the width of the waveguides and the length L of the directional couplers. The width $w \in [1,\ 1.15]\,\mu$m, the gaps $g_1,\ g_2 \ldots\ g_n \in [1,\ 1.3]\,\mu$m and the length $L \in [0,\ 2400]\,\mu$m. The width range is chosen such that the waveguide always remains single mode. The width and thickness variations caused by the imperfect fabrication process are denoted by $[\Delta w, \Delta t]$. For this process $\Delta w \in [-0.1\ 0.1]\,\mu$m and $\Delta t \in [-3\ 3]$ nm. The radius of the ring section is fixed at $R = 600\,\mu$m for all the rings. The length L for each ring is kept the same so that the round trip length, given the fixed radius, is the same for all rings. This is needed in order to ensure that the rings in the filter have the same free spectral range.

The set of design variables (control variables) is denoted by $\mathbf{x}_d$, while the set of parametric uncertainties (environment variables) is represented by $\mathbf{x}_e$.

The filter performance should be robust with respect to the parametric uncertainties which impact the cross-sectional geometry, i.e. width and thickness variation. This involves finding the right combination of the design variables that leads to the most robust design.

Computing the response at the Through or Drop port basically involves simple linear algebra and matrix manipulation once the power coupling ratio is known for each coupler section [17]. Let P_{L0} represent the power coupling ratio when $L = 0\,\mu$m. We denote the beat length, i.e. the coupling length needed to completely couple light from the first waveguide into the second waveguide and back into the first waveguide, by L_π. Computing the power coupling ratio of a directional coupler, given a length L and a certain geometry for the cross-section, can be time consuming, as computation of P_{L0} and L_π requires numerical simulation. A commercial electromagnetic solver, PhoeniX Software [20], is used to simulate both quantities. A coupled mode theory model [21] is employed to simulate P_{L0}. On the other hand, L_π is found using a mode solver. Both simulations require approximately 10 minutes.

Once P_{L0} and L_π are known for a given geometry, the power coupling ratio for any length L is cheap to compute. This is because the coupled power as a function of coupling length follows a sinusoidal curve whose period is given by L_π [22]. The fidelity of the beat length L_π simulated via the mode solver was independently verified by simulating a directional coupler with different coupling lengths using the coupled mode theory model [21]. The resulting power coupling ratios were used to fit the sinusoidal curve of power coupling ratio with respect to coupling length. The period of this curve (i.e. the fitted beat length) was compared to the mode solver simulated beat length. The two different simulated beat length values showed strong correspondence. Therefore, the mode solver is used to simulate the beat length L_π in this work. The scattering matrix analysis [17] that follows [17] the computation of P_{L0} and L_π in order to find the serial ring resonator response is not computationally expensive.

We therefore make a clear distinction between the computationally expensive and cheap parts of the system. We construct metamodels of the expensive components, i.e. response of P_{L0} and L_π, given the design variables and the parametric uncertainties. The power coupling ratio given by the combination of the cheap models is then used as an input to the scattering matrix analysis [17] in order to get the system response for the serial ring resonator. This involves the calculation of the phase factor describing the propagation inside the ring,

$$\theta = n_{\text{eff}} \frac{2\pi}{\lambda} T_L \tag{1}$$

where T_L is the total round trip length in the ring, while n_{eff} is the effective index. The phase factor is used together with the power coupling ratio for each coupler section to derive a 2×2 transfer matrix for each ring. The total transfer matrix is just the product of the N transfer matrices representing the N rings in the system. The elements of the total transfer matrix can then be used to compute the transfer function for the through port. Details for each individual step in this process can be found in [17].

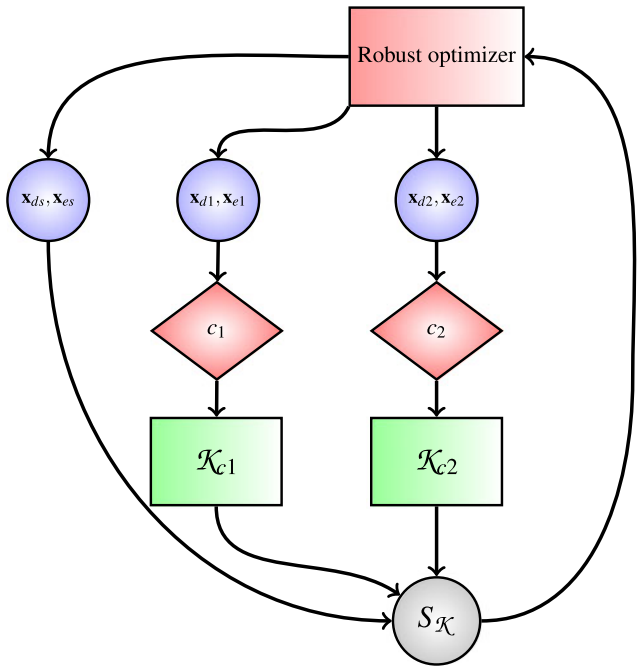

Fig. 2. The process of robust optimization of the approximate system response based on Kriging models of expensive components is shown.

Robust optimization can then be efficiently applied on the approximate system response. The robust optimum should converge to the solution that would have been found on the reference simulators. This convergence requires improvement of the cheap system response by adding more data points from the expensive simulation in strategically important regions until an initially specified budget for total simulations is exhausted. In what follows, we expand upon the robust optimization method and the proposed approach for adaptively improving the system response.

III. System Robust Optimization

Let $S_{\mathcal{K}}$ represent a system based on components c_1 to $c_{\mathcal{N}}$. Since the components are expensive to simulate, we construct Kriging metamodels $\mathcal{K}_{c1}$ to $\mathcal{K}_{c\mathcal{N}}$ of the components based on a set of simulated responses. Robust optimization is applied on the approximate system response generated from the underlying Kriging metamodels.

Fig. 2 visually depicts the relationship between the design variables, $\mathbf{x}_d$, the parametric uncertainties, $\mathbf{x}_e$, and the components, system response. Since we construct metamodels for only P_{L0} and L_π, Fig. 2 shows only two component metamodels $\mathcal{K}_{c1}$ and $\mathcal{K}_{c2}$. Once we have the cheap models for P_{L0} and L_π as a function of width, gap and thickness, the response for all the directional couplers in the serial ring resonator can be found since they share the same domain in the design variables $[w\ g_i]$ and the uncertainties $[\Delta w, \Delta t]$. Fig. 2 shows that some variables and uncertainties $(\mathbf{x}_{\text{ds}}, \mathbf{x}_{\text{es}})$ can directly impact the system

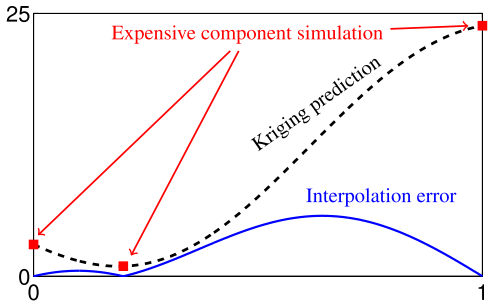

Fig. 3. Kriging model of a one-dimensional function based on three samples. The predicted Kriging mean squared error is also shown in the plot. As expected, the predicted error is zero at the sample points.

response $S_{\mathcal{K}}$. For the serial ring resonator problem, the length L is a system level design variable since it does not impact the response of P_{L0} and L_{π}, but it has an influence on the system response.

The robust optimizer operates on the system response $S_{\mathcal{K}}$ and tries to find a relatively insensitive solution by optimizing the design variables. The system level robust optimization problem in general may be expressed as,

$$\min_{\mathbf{x}_d \in \mathbb{X}_d} \max_{\mathbf{x}_e \in \mathbb{X}_e} S_{\mathcal{K}}(\mathcal{K}_{c1}(\mathbf{x}_{d1}, \mathbf{x}_{e1}), \mathcal{K}_{c2}(\mathbf{x}_{d2}, \mathbf{x}_{e2}) \ldots, \mathcal{K}_{c\mathcal{N}}(\mathbf{x}_{d\mathcal{N}}, \mathbf{x}_{e\mathcal{N}}), \mathbf{x}_{\mathrm{ds}}, \mathbf{x}_{\mathrm{es}}) \quad (2)$$

where $\mathbf{x}_{d1}$ to $\mathbf{x}_{d\mathcal{N}}$ are the design variables of component metamodel $\mathcal{K}_{c1}$ to $\mathcal{K}_{c\mathcal{N}}$. The parametric uncertainties $\mathbf{x}_{e1}$ to $\mathbf{x}_{e\mathcal{N}}$ affect the component metamodels $\mathcal{K}_{c1}$ to $\mathcal{K}_{c\mathcal{N}}$, respectively. The design variables $\mathbf{x}_{\mathrm{ds}}$ and the parametric uncertainties $\mathbf{x}_{\mathrm{es}}$ directly affect the system response, see Fig. 2. $\mathbb{X}_d$ and $\mathbb{X}_e$ are the domains for $\mathbf{x}_d$ and $\mathbf{x}_e$, respectively. Equation (2) shows that the robust optimization problem is a nested optimization problem where the objective of the outer minimization itself involves an inner global maximization. This fact means that the efficient use of metamodeling techniques is essential to determine robust designs at affordable computational costs.

IV. Adaptive Improvement of Approximate System

A. Component Metamodels: Kriging

Kriging is an interpolation technique with a statistical basis [2]. An important property of Kriging is that it provides an estimate for the interpolation error. Fig. 3 shows a Kriging metamodel of a one-dimensional function based on three samples of a reference function. The black dashed line is the predicted Kriging interpolation $\hat{y}$. The figure also shows the predicted interpolation error, s^2, given by the solid blue line. The interpolation error is zero at the sample points and increases as the distance between the sample points increases.

The combination of the Kriging prediction $\hat{y}$ and the interpolation error, s^2, can be used to iteratively improve the metamodel so that the minimum of the expensive function is found efficiently. Jones *et al.* [23] devised such a method for adaptively improving the metamodel in regions of interest for optimization. The method assumes that the metamodel uncertainty in the response, $\hat{y}$, at any position $\mathbf{x}$ in the domain can be modeled as a normal random variable with mean $\hat{y}$ and variance s^2, Fig. 4.

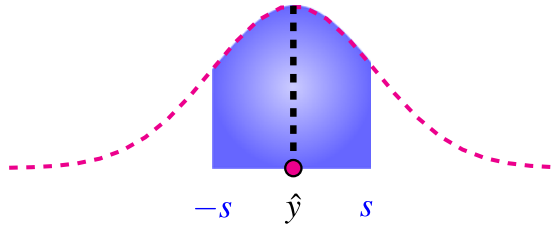

Fig. 4. An example of a normally distributed random variable which models the uncertainty in the Kriging prediction $\hat{y}$ for a given location x. The variance of the random variable is given by the Kriging mean squared error s^2.

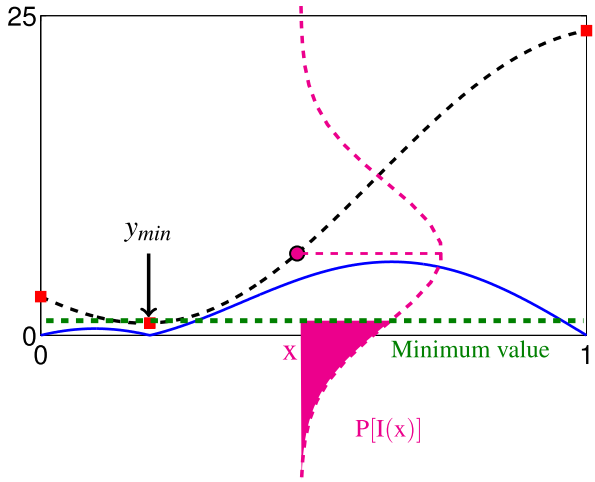

Fig. 5. The probability of improvement over the minimum observed response $y_{\min}$ is shown for a certain location in the design domain.

Fig. 5 shows this random variable superimposed on the Kriging prediction curve. The area shaded in pink quantifies the predicted probability of improvement over the current observed minimum, $y_{\min}$, if an expensive simulation is performed for that location. If we take the first moment of area of the shaded region, we get the *expected* improvement over $y_{\min}$. By maximizing the expected improvement (EI) criterion for the whole domain, a sampling location is found that provides the highest predicted improvement over $y_{\min}$. Performing EI maximization over several iterations, with a new simulation point corresponding to the maximum EI value added at each iteration, enables the global minimum to be found efficiently.

B. System Level Robust Expected Improvement

The authors extended efficient global optimization (EGO) approach suggested by Jones *et al.* to the system level [24]. We proposed an approach for robust optimization of a system based on component metamodels, and verified it on different problems. A system level robust expected improvement criterion was derived which enabled iterative sampling of the expensive components such that the system robust optimum was found efficiently. Here we summarize the main steps of the method, for detailed derivation the reader is referred to [24].

To derive the system level robust EI criterion, a system level error estimate in the approximate system response $S_{\mathcal{K}}$ is needed. In order to find a system level error estimator $s_{\rm sys}$, a linear Taylor series expansion of $S_{\mathcal{K}}$ was performed.

Let $r_{\mathcal{K}}^{\rm sys}$ represent the best worst-case cost on the system response, determined using Equation (2). To improve over $r_{\mathcal{K}}^{\rm sys}$ a location is sought that could potentially have a lower *worst-case* cost. Let $\hat{y}_{\rm sys}^{\max}(\mathbf{x}_d)$ represent the worst-case cost for a given value of $\mathbf{x}_d$,

$$\hat{y}_{\rm sys}^{\max}(\mathbf{x}_d) = \max_{\mathbf{x}_e \in \mathbb{X}_e} S_{\mathcal{K}}. \tag{3}$$

The corresponding location in $\mathbb{X}_e$ where the worst-case cost is obtained is given by $\mathbf{x}_e^{\max}$.

The derived system level error estimator $s_{\rm sys}$ was used in combination with the system response, $\hat{y}_{\rm sys}$, to give infill sampling criteria in the design variable range $\mathbb{X}_d$ and parametric uncertainties range, $\mathbb{X}_e$. A system level robust expected improvement criterion was developed in $\mathbb{X}_d$ to suggest locations with the highest expectation of improving over the current robust optimum $r_{\mathcal{K}}^{\rm sys}$

$$\begin{aligned}\mathrm{EI}_{\mathrm{sys},d}(\mathbf{x}_d) = \; & (r_{\mathcal{K}}^{\rm sys} - \hat{y}_{\rm sys}^{\max})\Phi\left(\frac{r_{\mathcal{K}}^{\rm sys} - \hat{y}_{\rm sys}^{\max}}{s_{\rm sys}^{\max}}\right) \\ & + s_{\rm sys}^{\max}\phi\left(\frac{r_{\mathcal{K}}^{\rm sys} - \hat{y}_{\rm sys}^{\max}}{s_{\rm sys}^{\max}}\right).\end{aligned} \tag{4}$$

On the other hand, a system level worst-case expected deterioration criterion was developed for the parametric uncertainty space $\mathbb{X}_e$ which suggested locations with the highest expectation of deterioration in the worst-case system response at $\mathbf{x}_d^{\rm new}$

$$\begin{aligned}\mathrm{ED}_{\mathrm{sys},e}(\mathbf{x}_d^{\rm new}, \mathbf{x}) = \; & (\hat{y}_{\rm sys} - g_{\mathcal{K}}^{\rm sys})\Phi\left(\frac{\hat{y}_{\rm sys} - g_{\mathcal{K}}^{\rm sys}}{s_{\rm sys}}\right) \\ & + s_{\rm sys}\phi\left(\frac{\hat{y}_{\rm sys} - g_{\mathcal{K}}^{\rm sys}}{s_{\rm sys}}\right).\end{aligned} \tag{5}$$

The combination of $\mathrm{EI}_{\mathrm{sys},d}$ and $\mathrm{ED}_{\mathrm{sys},e}$ can be used to suggest a sampling location in $\mathbb{X}_d$ and $\mathbb{X}_e$, respectively. To do this, the maximum for $\mathrm{EI}_{\mathrm{sys},d}$ and $\mathrm{ED}_{\mathrm{sys},e}$ in the respective domains $\mathbb{X}_d$ and $\mathbb{X}_e$ is found. This is the location at which the response is evaluated on the expensive simulation. New component metamodels are constructed with the augmented set of samples and responses. The process of maximizing $\mathrm{EI}_{\mathrm{sys},d}$, $\mathrm{ED}_{\mathrm{sys},e}$ and sampling the expensive simulation is repeated until the total number of expensive simulations are exhausted. At this point, the location for the robust optimum, $r_{\mathcal{K}}$, found at the last iteration is returned as the final solution. Details related to the derivation and the actual algorithm may be found in [24].

V. Results

The algorithm is demonstrated on second order and third order TripleX based ring resonators. The objective is a bandpass filter response at the Through port. Let $H(n_f)$ represent the spectral response at the Through port. We normalize the frequency with respect to the free spectral range of the serial ring resonator, which is calculated given the operating wavelength of 637 nm. For the normalized frequency $n_f \in [0\ 1]$, the aim is to achieve complete rejection in the stop-bands range $[0\ 0.1]$, $[0.9\ 1]$ and allow power to pass in the pass-band range $[0.2\ 0.8]$. Strictly, a bandpass filter should ideally pass all frequencies in a certain range and reject frequencies outside that range. However, since we are considering only low (second and third) order filters in this work, the frequency ranges $[0.1\ 0.2]$ and $[0.8\ 0.9]$ are reserved for the slow roll-off.

The robust optimization problem may be written as,

$$\begin{aligned}\min_{w,\mathbf{g},L}\max_{\Delta w,\Delta t} \quad & \frac{1-b}{2}\|\bar{H}_{\rm stop1}\|_p + b[1 - \|1 - \bar{H}_{\rm pass}\|_p] \\ & + \frac{1-b}{2}\|\bar{H}_{\rm stop2}\|_p,\end{aligned} \tag{6}$$

where $\bar{H}_{\rm stop1}$, $\bar{H}_{\rm pass}$, and $\bar{H}_{\rm stop2}$ represent the vector of responses for the normalized frequencies $n_f \in [0\ 0.1]$, $n_f \in [0.2\ 0.8]$, and $n_f \in [0.9\ 1]$, respectively. We take the p-norm of the vector of responses, $\bar{H}_{\rm stop1}$ and $\bar{H}_{\rm stop2}$, in the stop bands. The p-norm approximates the maximum value for $\bar{H}_{\rm stop1}$ and $\bar{H}_{\rm stop2}$ in the respective stop band ranges. For the pass band, the p-norm is used to approximate the minimum value for $\bar{H}_{\rm pass}$ in $n_f \in [0.2\ 0.8]$. The sum found is dependent on the weight b. In this work, we choose $b = 0.6$ and $p = 20$. The objective in Eq. (6) is basically a weighed sum of the approximate maximum in $\bar{H}_{\rm stop1}$, $\bar{H}_{\rm stop2}$ and the approximate minimum in $\bar{H}_{\rm pass}$. The robust optimization involves finding the best worst-case cost of this weighed sum.

The robust optimum is compared against the optimal solution found when the uncertainties are not part of the optimization problem. Equation (7) shows the nominal optimization problem definition,

$$\begin{aligned}\min_{w,\mathbf{g},L} \quad & \frac{1-b}{2}\|\bar{H}_{\rm stop1}\|_p + b[1 - \|1 - \bar{H}_{\rm pass}\|_p] \\ & + \frac{1-b}{2}\|\bar{H}_{\rm stop2}\|_p.\end{aligned} \tag{7}$$

In the above problem the weighed sum is simply minimized with respect to the design variables $w, \mathbf{g}, L$ without considering the impact of the uncertainties.

The algorithm is demonstrated by applying it on a second order and third order serial ring resonator. The robust solution is compared against the deterministic optimum. The optimal locations found on the cheap system response are also fed into the expensive electromagnetic simulators as a postprocessing step in order to verify the fidelity of the solution.

For deterministic optimization, it was assumed that the ring resonator structure is symmetric. This means that in the case of second order resonator $g_3 = g_1$. Similarly, for the third order resonator, $g_4 = g_1$ and $g_3 = g_2$. For robust optimization both the cases, one assuming symmetry and another without symmetry of the gaps, were considered. It was found that for both cases, the best worst-case objective obtained was relatively the same. Therefore, the greater flexibility of choosing unsymmetrical gap values does not automatically lead to a greater chance of a better solution. In this scenario, it makes sense to perform robust optimization using symmetric gaps, since this reduces the total number of design variables in the problem. In this work, the robust optimization results shown are based on symmetric resonators.

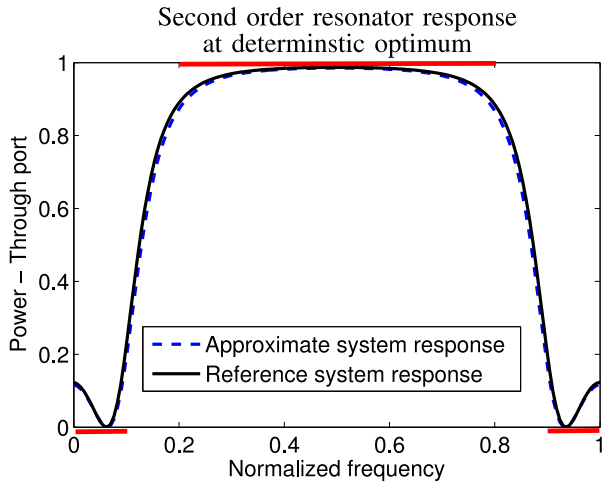

Fig. 6. Comparison of the approximate system response and the reference system response is shown for the solution obtained by the deterministic optimization algorithm.

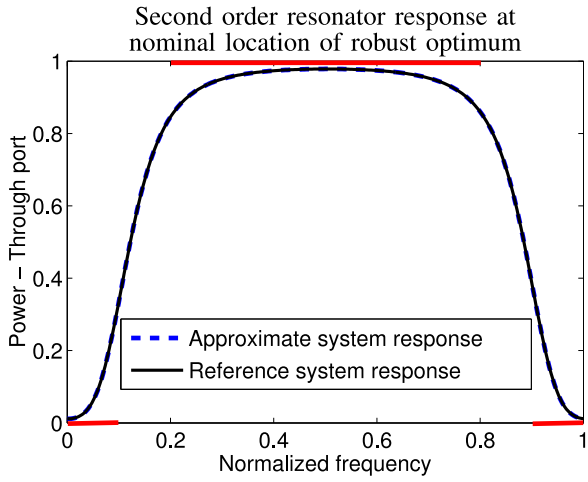

Fig. 7. Comparison of the approximate system response and the reference system response is shown at the nominal location of the robust optimum.

A. *Second Order Serial Ring Resonator*

Robust optimization is applied on the cheap system response of the second order resonator. The approximate response is generated by applying scattering matrix analysis [17] on the power coupling ratio for each directional coupler found via the component metamodels for P_{L0} and L_π. The robust optimization algorithm is started by constructing the initial component metamodels for P_{L0} and L_π. The metamodels are built based on 60 initial expensive simulations of the coupled mode theory model (P_{L0}) [21] and the mode solver (L_π). The locations for the design variables w, g and the uncertainties $[\Delta w\ \Delta t]$ is chosen in the combined design variable and uncertainties space. The initial locations are chosen via Latin Hypercube sampling (LHS) [25], a type of Design of Experiments. Since L is a system level design variable, it does not have to be sampled.

The algorithm is allowed a total computational budget of 240 expensive simulations for both P_{L0} and L_π. This means the method can run for 60 iterations, since three such simulations are run at each iteration for the three different gaps g_1, g_2 and g_3.

A system level deterministic optimization algorithm [26] is applied on the problem for comparison with the robust solution. The approach is also based on adaptive improvement of component metamodels. Since uncertainties are not included in the problem definition in the deterministic case, the total number of variables is only limited to the design variables w, $\mathbf{g}$, and L. A total computational budget of 60 expensive simulations is available. The initial metamodels for P_{L0} and L_π are constructed based on 10 locations for w and g chosen via LHS. Note that due to the lower dimensionality of the deterministic problem, fewer samples are needed compared to the robust case.

The approximate system response based on the component metamodels for P_{L0} and L_π is plotted in Fig. 6 at the deterministic optimum. The normalized frequency is plotted on the x-axis. The actual center frequency will in fact deviate from the original position because of a change in the waveguide width or thickness. Therefore the original frequency has not been provided in the x-axis (the central frequency can be different for the robust and nominal solution). It should be pointed out here

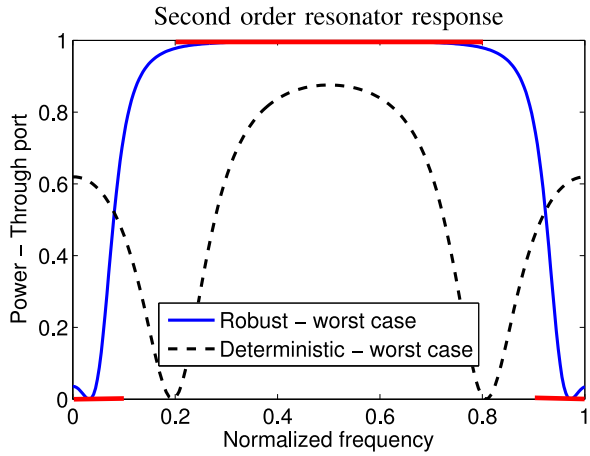

Fig. 8. Spectral response at the Through port of the second order serial ring resonator for the deterministic and the robust optimum, assuming that the worst-case fabrication error is realized.

that we are interested in the bandpass performance and not in the absolute value of the frequency/wavelength at which it takes place. The system response at the deterministic optimum based on simulation of P_{L0} and L_π on the actual simulator, PhoeniX Software [20], is also plotted. As expected, the approximate system response is quite close to the reference solution.

The same comparison is plotted for the robust optimum at the nominal location. Once again, the solution found on the actual simulator is quite similar to the approximate system response. This shows that the component metamodels predict P_{L0} and L_π with high fidelity in the neighborhood of the robust optimum. Comparing Fig. 7 with Fig. 6 it may appear that the robust solution is a better solution at the nominal location than the deterministic optimum in Fig. 6. However, the numerical objective value for the deterministic optimum is lower than it is for the robust optimum since the highest value in both the stop bands is lower for the deterministic optimum than the corresponding highest value in the stop bands for the robust solution.

Fig. 8 shows the comparison of the deterministic (dashed black line) and the robust optimal solution (solid blue line)

TABLE I
A COMPARISON OF THE ROBUST AND NOMINAL OPTIMA FOR THE SECOND ORDER AND THE THIRD ORDER FILTERS IS GIVEN

Optimum	w	g_1	g_2	g_3	g_4	L	Δw	Δt	Nominal	Worst-case
Nominal second order	1.1250	1.1321	1.1122	1.1321		1897.7	−0.0268	−0.0027	0.0166	0.7545
Robust second order	1.0731	1.00	1.2715	1.00		130.299	−0.0168	0.003	0.0645	0.2274
Nominal third order	1.0746	1.1583	1.1796	1.1796	1.1583	2390.9	0.1	0.0027	0.0089	0.8975
Robust third order	1.1356	1.0190	1.2990	1.2990	1.0190	230.573	0.1	−0.003	0.0255	0.1510

assuming that the worst-case fabricated structure is realized. The ideal band-pass response is indicated in red. The figure shows that, for the worst possible changes in ΔW and Δt, the filter performance for the deterministic optimum deteriorates dramatically. A significant portion of light is passing through in the stop bands and there is very little attenuation. Although, the filter still passes some light in the pass band, the performance is significantly worse compared to the performance at the nominal location, Fig. 6.

In comparison, the worst-case solution for the robust filter (solid blue line) gives much better performance in the pass band, since all the light is allowed to pass in the range of frequencies between $n_f \in [0.2\ 0.8]$. The filter performance could be better since the frequencies in the stop band are not completely attenuated. The slow roll off means that a large amount of light is still being passed through in the regions of the stop bands that are closer to the pass band. However, it should be stressed that this is the worst possible filter performance that can be realized at the robust optimum assuming that structure is fabricated in a way that is most detrimental to the filter performance. For any other fabrication error in thickness and width, the performance would be better than the solution provided in the figure.

B. Third Order Serial Ring Resonator

The deterministic and robust optimization algorithms are applied on a third order resonator as well. The same computational budget is allocated for both problems as was used for the second order resonator problem. We do not need to increase the computational budget since the underlying component metamodels are made for a single directional coupler. That directional coupler response can be reused for all the directional couplers in the system since all the couplers share the same design variables and uncertainties domain. The order of the resonator can therefore be increased arbitrarily without incurring high computational costs. This scalability at low cost is one of the primary attractions of the system based approach described in this work.

Fig. 9 compares the worst-case filter performance for the deterministic and robust optimum. There is hardly any rejection of frequencies in the stop bands for the deterministic optimum (dashed black line). The pass band performance is significantly better than the deterministic optimum for the second order resonator, Fig. 8. On the other hand, the worst-case filter response for the robust optimum shows much better attenuation of the light in the stop band. The performance for the robust optimum in the stop bands is also much better than the corresponding result for the robust optimum on the second order ring resonator,

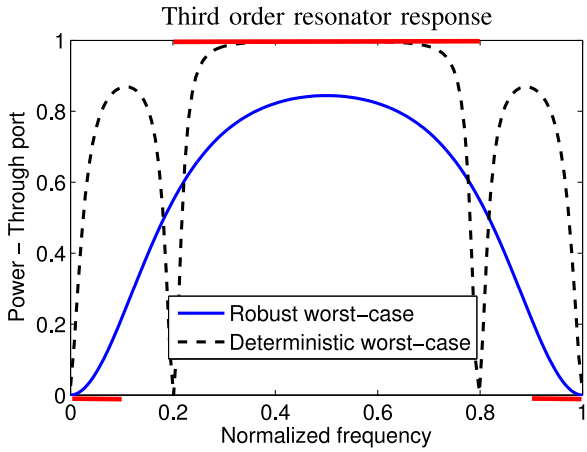

Fig. 9. Spectral response at the Through port of the third order serial ring resonator for the deterministic and the robust optimum, assuming that the worst-case fabrication error is realized.

Fig. 8. However, the pass-band performance of the filter for the robust solution is far from ideal since quite a lot of power is lost.

Table I shows a numerical comparison of the second order and third order nominal and robust designs. The optimal design variable locations for w, $\mathbf{g}$, L are given in columns 2–7. Columns 8 and 9 provide the location for the fabrication uncertainties $[\Delta w\ \Delta t]$ at which the worst-case filter performance is found for the different optima. The last two columns give the numerical performance at the nominal and the worst-case location for the second and third order nominal and robust optimal solutions.

Turning our attention to the objective value at the nominal location, second last column in Table I, we note that the nominal optimum provides a better (lower) solution for both the second and the third order resonators than the robust optimum. However, if the worst possible fabrication with respect to the objective were to occur, then the robust optimal solution deteriorates much less than the nominal solution for both the second and the third order ring resonators, last column. This indicates that, even if the robust optimum is nominally suboptimal, it performs much better in the worst-case than the nominal solution. As expected, the numerical solution for the robust optimum of the third order filter is better than the robust solution for the second order filter. If higher order filters were robustly optimized, the best worst-case filter performance could further improve. Note that the same cannot be said for the deterministic optimum.

Columns 8 and 9 show the value for $[\Delta w\ \Delta t]$ at which the worst-case response was found. Apart from the worst-case location for the robust optimum of the third order ring resonator,

all the other worst-case locations occur in the interior of the uncertainty set.

VI. Conclusion

A robust optimization method for efficiently designing manufacturable serial ring resonators has been proposed in this work. The method is based on an iterative optimization strategy that optimizes an approximate system response based on mathematical modeling of the components built using Kriging. The approach is scalable since it depends on constructing mathematical models of the directional coupler section and using them to produce the serial ring resonator response instead of building new inexpensive models of every new serial ring resonator that is considered.

It was shown via examples of second order and third order TripleX based serial ring resonators that the approach can efficiently and consistently find a robust design that is relatively insensitive to fabrication deviations. In this example, the robust design showed a lower nominal performance, but a significantly better worst-case performance. In practice, this would translate into substantially higher yields on optical filters optimized for robustness. Since the method is based on constructing metamodels of black-box components, it is envisaged that the technique can potentially be employed for efficient global robust optimization of other integrated photonic systems. The broader applicability of the proposed technique for system robust optimization should be investigated by applying it on other integrated photonic systems, e.g., Array Waveguide Gratings or interferometers based on MMI couplers.

References

[1] S. P. Gurav, K. Vervenne, H. J. Damveld, and A. van Keulen, "Bounded-but-unknown uncertainties in design optimization by combining the multipoint approximation method and design sensitivities," presented at the 43rd AIAA/ASME/ASCE/AHS/ASC Structures Structural Dynamics Materials Conf., Denver, CO, USA, Apr. 22–25, 2002, number AIAA-2002-1759.

[2] J. Sacks, W. Welch, T. J. Mitchell, and H. P. Wynn, "Design and analysis of computer experiments," *Statist. Sci.*, vol. 4, no. 4, pp. 409–435, 1989.

[3] S. Ur Rehman, M. Langelaar, and F. Van Keulen, "Robust optimization of 2×2 multimode interference couplers with fabrication uncertainties," *Proc. SPIE*, vol. 8627, pp. 862711–862713, 2013.

[4] S. Rehman, M. Langelaar, and F. Van Keulen, "Robust optimization of 2×2 multimode interference coupler affected by parametric uncertainties," presented at the 18th Annu. Symp. IEEE Photonics Society Benelux, Eindhoven, The Netherlands, 2013.

[5] S. Ur Rehman and M. Langelaar, "Efficient global robust optimization of unconstrained problems affected by parametric uncertainties," *Structural Multidisciplinary Optimization*, vol. 52, no. 2, pp. 319–336, 2015.

[6] A. Melloni, G. Cusmai, and F. Morichetti, "Design on tolerances in integrated optics," in *Proc. 14th Eur. Conf. Integr. Opt. Tech. Exhib., Contributed Invited Papers*, Eindhoven, The Netherlands, 2008, pp. 205–208.

[7] C. Vázquez, A. Tapetado, J. Orcutt, H. C. Meng, and R. Ram, "Tolerance analysis for efficient MMI devices in silicon photonics," *Proc. SPIE*, vol. 89900, pp. 89900A-1–89900A-7, 2014.

[8] J. J. G. M. van der Tol, M. Felicetti, and M. K. Smit, "Increasing tolerance in passive integrated optical polarization Converters," *J. Lightw. Technol.*, vol. 30, no. 17, pp. 2884–2889, Sep. 2012.

[9] K. Worhoff, P. V. Lambeck, and A. Driessen, "Design, tolerance analysis, and fabrication of silicon oxynitride based planar optical waveguides for communication devices," *J. Lightw. Technol.*, vol. 17, no. 8, pp. 1401–1407, Aug. 1999.

[10] D. Pérez-Galacho, R. Halir, A. Ortega-Moñux, C. Alonso-Ramos, R. Zhang, P. Runge, K. Janiak, H.-G. Bach, A. G. Steffan, and Í. Molina-Fernández, "Integrated polarization beam splitter with relaxed fabrication tolerances," *Opt. Express*, vol. 21, no. 12, pp. 14146–14151, Jun. 2013.

[11] C. Alonso-Ramos, R. Halir, A. Ortega-Moñux, P. Cheben, L. Vivien, I. Molina-Fernández, D. Marris-Morini, S. Janz, D.-X. Xu, and J. Schmid, "A general approach for robust integrated polarization rotators," *Proc. SPIE*, vol. 8781, pp. 8781-1–8781-9, 2013.

[12] R. Wu, C.-H. Chen, C. Li, T.-C. Huang, F. Lan, C. Zhang, Y. Pan, J. E. Bowers, R. G. Beausoleil, and K.-T. Cheng, "Variation-aware adaptive tuning for nanophotonic interconnects," in *Proc. IEEE/ACM Int. Conf. Computer-Aided Design*, Piscataway, NJ, USA, 2015, pp. 487–493.

[13] J. W. Bandler *et al.*, "Space mapping: The state of the art," *IEEE Trans. Microw. Theory Techn.*, vol. 52, no. 1, pp. 337–361, Jan. 2004.

[14] A. Bekasiewicz, S. Koziel, and L. Leifsson, "Fast optimization of integrated photonic components using response correction and local approximation surrogates," *Procedia Comput. Sci.*, vol. 51, pp. 825–833, 2015.

[15] R. Heideman, M. Hoekman, and E. Schreuder, "TriPleX-based integrated optical ring resonators for lab-on-a-chip and environmental detection," *IEEE J. Sel. Topics Quantum Electron.*, vol. 18, no. 5, pp. 1583–1596, Sep./Oct. 2012.

[16] C. J. Kaalund and G.-D. Peng, "Pole-zero diagram approach to the design of ring resonator-based filters for photonic applications," *J. Lightw. Technol.*, vol. 22, no. 6, pp. 1548, Jun. 2004.

[17] O. S. Ahmed, M. A. Swillam, M. H. Bakr, and X. Li, "Efficient design optimization of ring resonator-based optical filters," *J. Lightw Technol.*, vol. 29, no. 18, pp. 2812–2817, Sep. 2011.

[18] A. Melloni, "Synthesis of a parallel-coupled ring-resonator filter," *Opt. Lett.*, vol. 26, no. 12, pp. 917–919, 2001.

[19] C. K. Madsen, "General IIR optical filter design for WDM applications using all-pass filters," *J. Lightw. Technol.*, vol. 18, no. 6, pp. 860–868, Jun. 2000.

[20] PhoeniX Software, "PhoeniX Software 4.8.4," 2014.

[21] K. R. Hiremath, R. Stoffer, and M. Hammer, "Modeling of circular integrated optical microresonators by 2-D frequency domain coupled mode theory," *Opt. Commun.*, vol. 257, no. 2, pp. 277–297, 2006.

[22] R. R. A. Syms and J. R. Cozens, *Optical Guided Waves and Devices*. London, U.K.: McGraw-Hill, 1992.

[23] D. R. Jones, M. Schonlau, and W. J. Welch, "Efficient global optimization of expensive black-box functions," *J. Global Optimization*, vol. 13, no. 4, pp. 455–492, 1998.

[24] S. Ur Rehman and M. Langelaar, "Infill sampling criterion for global robust optimization of systems with independent components," *Eng. Optimization*, to be published.

[25] M. Morris and T. J. Mitchell, "Exploratory designs for computational experiments," *J. Statist. Planning Inference*, vol. 43, no. 3, pp. 381–402, 1995.

[26] S. Ur Rehman and M. Langelaar, "Adaptive efficient global optimization of systems with independent components," *Struct. Multidisciplinary Optimization*, to be published.

Samee Ur Rehman received the M.Sc. degree in electrical engineering from the Jacobs University, Bremen, Germany, in 2011. In 2010, he worked at the German Research Center for Artificial Intelligence, Bremen, Germany. He received the Ph.D. degree from the Delft University of Technology, Delft, The Netherlands, in 2016. He is currently working as a Design Engineer at ASML, The Netherlands. His research interests include system optimization, deterministic and robust optimization, metamodelling, and their application to optics and electromagnetics.

Matthijs Langelaar received the M.Sc. degree in mechanical engineering from the Twente University, Enschede, The Netherlands, in 1999. He recieved the Ph.D. degree from the Delft University of Technology, Delft, Germany, in 2006. He worked as a Researcher at the Robotics Institute, German Aerospace Agency, Germany. He is currently working as an Assistant Professor at the Delft University of Technology. His research interests include design optimization, with particular focus on topology optimization and surrogate-based robust optimization.